

# An Examination of Seismic Responses of Soft Grounds and a Highway Embankment in 2003 Tokachi-Oki Earthquake

**S. Nishimoto & T. Egawa**

*Civil Engineering Research Institute for Cold Region, PWRI, Sapporo, JAPAN*

**T. Ikeda**

*Research Institute of Technology, Tobishima Corporation, Noda, JAPAN*



## SUMMARY:

Liquefaction array observations have been conducted on soft ground in Tomakomai, Hokkaido, and on a highway embankment built there for the purpose of verifying the seismic performance of such embankments on soft ground and developing anti-seismic technologies. Since the start of soft-ground observations in 1990, data from 17 earthquakes have been obtained, and the complex seismic behavior of soft ground associated with the related nonlinear characteristics has been clarified. Seismic observation of the highway embankment was started in 1996, and a variety of amplitude values have been recorded with maximum accelerations ranging from less than  $10 \text{ cm/s}^2$  to more than  $100 \text{ cm/s}^2$ . These data were used to examine the seismic nonlinear behavior of the highway embankment. The results showed that nonlinear characteristics were observed in the seismic behavior of the ground and the embankment, and that the low-order natural frequencies of both were almost the same.

*Keywords: seismic observation, soft ground, road embankment, nonlinearity*

## 1. INTRODUCTION

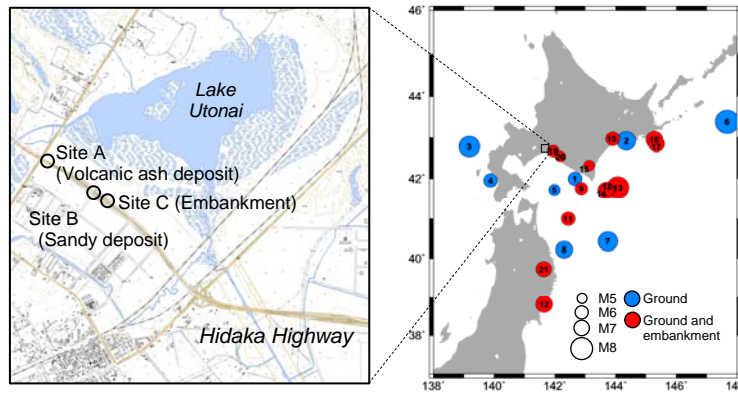
Liquefaction array observations have been conducted on soft ground in Tomakomai, Hokkaido, and on a highway embankment built there with the aim of determining the effectiveness of liquefaction countermeasures and verifying the seismic performance of the embankment. So far, data on seismic ground motion ranging from minor movement with a maximum acceleration of less than  $10 \text{ cm/s}^2$  to a level just before nonlinear behavior occurred have been recorded (Hayashi et al., 2000, Nishikawa et al., 2001, Nishikawa et al., 2002).

In the 2003 Tokachi-Oki Earthquake, a clear increase in pore water pressure and acceleration exceeding  $130 \text{ cm/s}^2$  were recorded (Nishimoto et al., 2006, Nishimoto et al., 2007). This paper discusses the seismic behavior of a highway embankment on soft ground from the general viewpoint of the relationship with nonlinear ground characteristics.

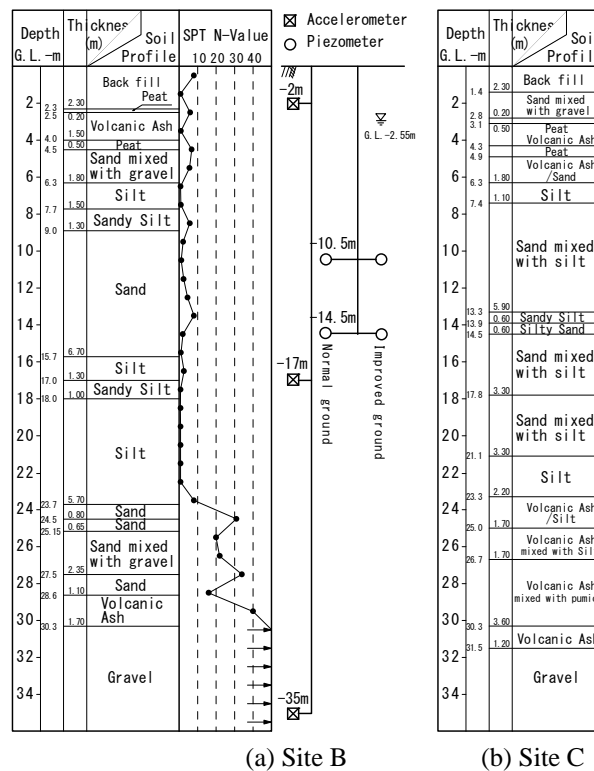
## 2. OVERVIEW OF LIQUEFACTION ARRAY OBSERVATIONS

Figure 2.1 shows the three study sites. Ground is observed in two locations (Site A and Site B), and embankment observation is performed in one location (Site C). At Site A, volcanic ash soil predominates, and at Site B sandy soil predominates. Site C is in the same region as Site B. In this study, sites B and C were examined. Figure 2.2 shows geological columns for these two locations and the positions where seismometers (accelerometers) and piezometers are installed at Site B. As loose sandy soil deposits are found in the subsurface layer at Site B, liquefaction is likely to occur when there is an earthquake in the region. For this reason, ground over an area measuring 15 m in width and 15 m in depth along both sides of the highway embankment was improved using the sand compaction pile method (Hayashi et al., 2000) (Figure 2.3).

Accelerometers are installed at three different depths near the surface (G. L.: -2 m) of unimproved ground where no liquefaction countermeasures have been taken, at a medium depth (G. L.: -17 m) and



**Figure 2.1** Location of observation sites and distribution of epicenters of the observed earthquakes



**Figure 2.2** Soil profile and instrumentation

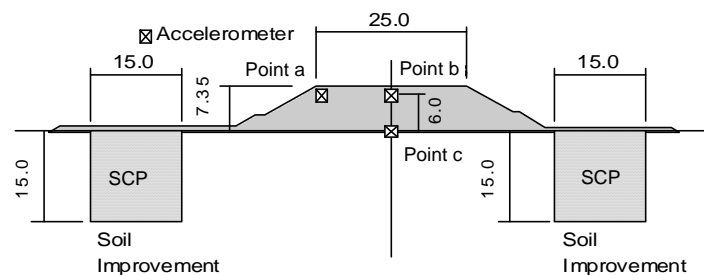


**Figure 2.3** Embankment profile and instrumentation (Site C)

in the bedrock (G. L.: - 35 m). The accelerometer at G. L. -35 m is located in a sandy gravel layer that spreads widely over surrounding areas and in which S-wave velocity exceeds 400 m/s. Piezometers are installed at two different depths: one in improved liquefiable ground and the other in unimproved ground.

The embankment observation site (Site C) is located approximately 50 m south of Site B (Fig. 2.4). Figure 2.3 shows the embankment configuration and the accelerometer installation positions. The accelerometers are installed at three points – in the embankment slope (Point a), at the center of the embankment crest (Point b) and at the bottom of the embankment (Point c). As the stratal organization of the surface ground at Site C is similar to that at Site B, and the two sites are located in the same region, it is considered that the seismic behavior of the embankment ground can be approximated by the behavior of sandy deposits. In this regard, the accelerometers in the embankment are linked with those in the sand deposits.

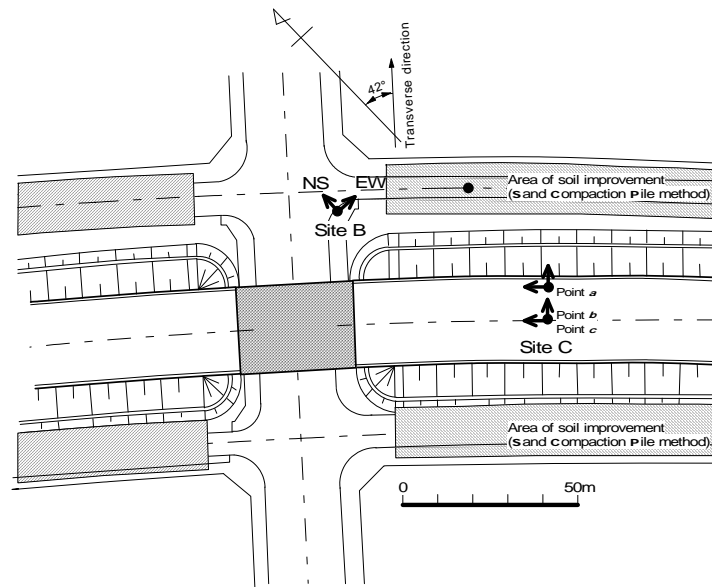


**Figure 2.4** Plan of observation sites of sandy soil ground (Site B) and embankment (Site C)

### 3. SEISMIC GROUND MOTION RECORDS OBTAINED VIA LIQUEFACTION ARRAY OBSERVATION DURING THE 2003 TOKACHI-OKI EARTHQUAKE

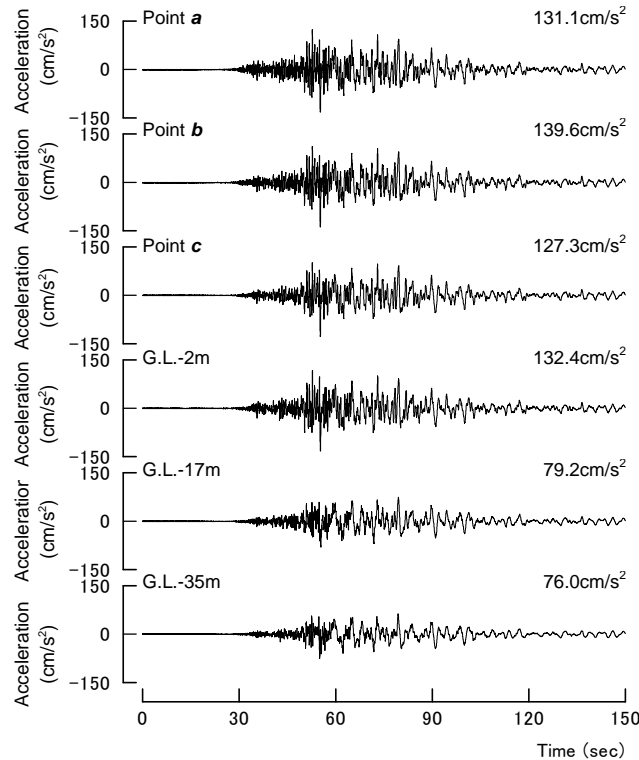
Since the start of soft-ground observation in 1990, data from 28 earthquakes had been recorded as of May 2011. Seismic observation of the highway embankment was commenced in 1996, and data from nine earthquakes have been collected. Table 3.1 shows details of these earthquakes and the maximum acceleration in the horizontal direction from the observed records, which include data from the 2003 Tokachi-Oki Earthquake that occurred at 4:50 on September 26, 2003, and its largest aftershock at 6:08 on the same day. The highest acceleration at the site was recorded on this day, and Figure 2.1 shows the epicenters (number 13 shows the main quake, and number 14 shows its largest aftershock). The distance from the observation point to the epicenter of the main quake was approximately 220 km, and the shortest distance to the fault was approximately 126.5 km.

Figure 3.1 shows acceleration in the transverse direction of the embankment at sites B and C as recorded during the 2003 Tokachi-Oki Earthquake. It can be seen that the tremor's motion arrived after approximately 30 seconds, and that principal motion with large amplitudes containing short-period components began after approximately 40 seconds. At around 55 seconds, components with longer periods became prominent, and motion consisting mainly of components with long periods continued after 70 seconds. This pattern was also seen at Site A.

The maximum acceleration was approximately  $76 \text{ cm/s}^2$  at G. L.  $-35 \text{ m}$  and approximately  $132 \text{ cm/s}^2$  at G. L.  $-2 \text{ m}$ , indicating amplification by a factor of approximately 1.7 in the soft ground surface layer. The maximum acceleration was approximately  $127 \text{ cm/s}^2$  at Point c (G. L.:  $\pm 0 \text{ m}$ ) on the bottom of the embankment and approximately  $138 \text{ cm/s}^2$  at Point b (G. L.:  $+6 \text{ m}$ ) on the embankment crest, indicating amplification from G. L.  $-35 \text{ m}$  to Point b by a factor of approximately 1.8 and from Point c to Point b by a factor of approximately 1.1. A similar pattern was also seen in the axial direction.

**Table 3.1 Profiles of earthquakes and observed records**

No	Profiles of Earthquakes				Maximum Acceleration (cm/s/s)																
	Region	Mj	Location	Depth (km)	Free Field (Upper : Site A , Bottom : Site B)									Embankment							
					G.L.-2m			G.L.-16m(Site A) G.L.-17m(Site B)			G.L.-35m			Point a		Point b		Point c			
	Date-Time	AX	TR	UD	AX	TR	UD	AX	TR	UD	AX	TR	UD	AX	TR	UD	AX	TR	UD		
Eq01	Uraga-Oki	6.3	41°59.8' 142°39.9'	64	10.7	13.7	4.4	8.8	8.6	6.7	8.1	3.9	-	-	-	-	-	-	-	-	-
					17.0	15.9	8.3	12.4	10.9	9.6	7.6	3.3	-	-	-	-	-	-	-	-	-
Eq02	Kushiro-Oki	7.5	42°55.0' 144°21.4'	101	-2)	-2)	-2)	-2)	-2)	-2)	-2)	-2)	-	-	-	-	-	-	-	-	-
					127.8	94.7	46.7	75.5	69.4	74.0	50.6	25.0	-	-	-	-	-	-	-	-	-
Eq03	Hokkaido-Nanseioki	7.8	42°46.8' 139°11.0'	35	13.0	15.8	6.1	10.7	12.4	8.8	10.8	4.6	-	-	-	-	-	-	-	-	-
					14.5	21.8	6.8	13.7	15.9	10.8	13.8	5.3	-	-	-	-	-	-	-	-	-
Eq04	Hokkaido-Nanseioki	6.3	41°57.3' 139°53.1'	24	6.0	11.2	2.5	4.1	6.0	3.4	4.1	2.3	-	-	-	-	-	-	-	-	-
					5.9	13.7	2.7	4.4	7.7	2.9	5.1	2.1	-	-	-	-	-	-	-	-	-
Eq05	Tomakomai-Oki	5.4	41°43.4' 141°59.3'	80	13.7	10.8	8.0	7.3	8.2	5.7	5.6	2.8	-	-	-	-	-	-	-	-	-
					-2)	-2)	5.1	8.5	8.8	10.3	8.7	2.5	-	-	-	-	-	-	-	-	-
Eq06	Hokkaido-Touhouki	8.2	43°22.3' 147°40.7'	28	47.2	47.1	24.8	22.7	29.0	19.8	20.8	11.2	-	-	-	-	-	-	-	-	-
					83.6	86.7	36.3	40.9	46.7	18.3	35.2	15.9	-	-	-	-	-	-	-	-	-
Eq07	Sanrikuharuka-Oki	7.6	40°25.6' 143°44.9'	0	44.8	79.7	10.0	31.6	38.5	24.4	25.9	7.7	-	-	-	-	-	-	-	-	-
					53.8	74.7	15.4	32.2	35.9	7.5	28.8	7.7	-	-	-	-	-	-	-	-	-
Eq08	Iwateken-Oki	7.2	40°13.2' 142°18.5'	48	18.7	23.3	4.9	9.4	12.6	7.9	11.5	3.8	-	-	-	-	-	-	-	-	-
					-2)	-2)	6.0	12.5	11.4	-2)	-2)	3.5	-	-	-	-	-	-	-	-	-
Eq09	Urakawa-Oki	5.9	41°45.4' 142°52.5'	49	-3)	-3)	-3)	-3)	-3)	-3)	-3)	-3)	6.1	7.2	4.8	6.2	7.1	4.7	4.7	5.1	2.8
					5.3	6.7	3.0	3.5	5.4	3.3	2.9	1.5	-	-	-	-	-	-	-	-	-
Eq10	Kushiro-Shicho-Nanbu	6.3	42°57.9' 143°54.5'	106	12.7	15.7	5.0	8.2	8.2	4.9	4.2	3.0	21.9	19.0	8.4	22.3	18.8	7.3	19.2	17.2	5.6
					-2)	-2)	5.5	11.3	10.4	8.6	6.1	3.3	-	-	-	-	-	-	-	-	-
Eq11	Aomori-ken-Touhouki	6.4	40°59.5' 142°26.4'	38	10.0	12.5	6.0	8.3	6.6	4.6	4.9	2.4	21.4	15.2	5.3	21.3	14.2	5.7	16.0	12.6	4.6
					22.1	13.7	6.8	12.8	9.3	10.5	5.6	2.6	-	-	-	-	-	-	-	-	-
Eq12	Myagiken-Oki	7.1	38°49.0' 141°39.2'	72	8.7	11.5	3.8	5.2	8.4	5.6	6.4	1.9	14.9	14.6	4.1	14.6	13.5	3.7	13.5	12.8	3.0
					15.9	13.1	3.4	9.4	8.7	6.1	6.3	2.3	-	-	-	-	-	-	-	-	-
Eq13	Tokachi-Oki	8.0	41°46.7' 144°4.7'	42	94.2	83.0	29.8	85.3	59.0	74.3	55.8	25.0	124.2	131.1	64.8	120.7	137.6	61.7	112.1	127.3	44.0
					127.0	132.4	53.6	74.4	79.2	69.7	76.0	25.7	-	-	-	-	-	-	-	-	-
Eq14	Tokachi-Oki	7.1	41°42.4' 143°41.7'	21	41.0	40.0	18.2	27.9	25.5	23.8	20.9	12.2	62.5	57.7	46.8	51.0	52.3	34.9	42.9	41.8	23.0
					57.9	49.0	31.6	41.8	39.3	29.0	25.8	15.5	-	-	-	-	-	-	-	-	-
Eq15	Tokachi-Shicho-Nanbu	5.2	42°19.1' 143°08.0'	48	-3)	-3)	-3)	-3)	-3)	-3)	-3)	-3)	19.7	16.8	8.8	16.2	14.1	6.5	9.6	9.8	4.4
					15.5	11.8	5.9	9.5	9.7	7.5	6.6	2.0	-	-	-	-	-	-	-	-	-
Eq16	Kushiro-Oki	7.1	42°56.6' 145°16.7'	48	12.8	22.7	4.7	9.0	11.6	8.5	6.9	4.1	15.8	23.2	7.7	15.8	22.4	7.8	15.0	21.2	7.1
					15.2	21.7	6.6	11.5	11.5	8.4	13.8	3.7	-	-	-	-	-	-	-	-	-
Eq17	Kushiro-Oki	6.9	41°43.9' 143°43.3'	46	14.3	11.3	4.3	9.0	7.5	7.0	5.6	4.1	20.3	19.9	5.3	19.9	19.4	5.8	19.4	17.5	5.3
					19.3	18.1	4.8	15.1	12.9	10.3	6.8	3.4	-	-	-	-	-	-	-	-	-
Eq18	Tokachi-Oki	6.1	41°43.9' 143°43.3'	40	7.5	8.4	3.2	6.4	5.0	5.6	4.0	2.8	8.6	9.0	4.1	8.5	8.9	4.4	8.3	8.6	4.3
					7.8	9.0	3.8	6.5	6.8	5.0	5.2	2.8	-	-	-	-	-	-	-	-	-
Eq19	Iburi-Shicho-Chutobu	5.6	42°40.2' 141°56.8'	126	12.2	10.4	12.1	8.5	6.8	6.5	5.0	4.4	14.9	10.4	19.2	14.6	9.9	16.5	9.3	8.6	8.6
					9.2	10.6	12.0	8.0	6.7	6.8	5.0	5.5	-	-	-	-	-	-	-	-	-
Eq20	Hidaka-Shicho-Seibu	4.9	42°32.3' 142°11.0'	125	6.6	19.5	8.2	6.5	8.4	4.1	6.1	3.4	12.5	9.9	17.3	10.2	9.3	16.0	9.9	8.0	10.8
					12.4	9.7	11.6	7.5	7.2	5.2	3.6	4.6	-	-	-	-	-	-	-	-	-
Eq21	Iwateken-Hokubui	6.8	39°43.9' 141°38.1'	108	11.1	14.0	6.4	6.1	8.7	4.9	6.2	2.7	18.6	16.5	11.9	16.7	13.4	10.0	12.6	11.9	6.0
					19.2	14.3	7.6	13.4	11.5	6.3	9.4	2.7	-	-	-	-	-	-	-	-	-



**Figure 3.1** Acceleration time histories of the 2003 Tokachi-Oki Earthquake at the Site B and C (in the direction transverse to the embankment axis)

## 4. EVALUATION OF EMBANKMENT NONLINEAR BEHAVIOR

### 4.1. Input motion and maximum response values

This section discusses the relationship between the maximum motion input to an embankment and the maximum response of the embankment in the transverse direction.

First, the relationship between input motion levels and the seismic behavior of ground was examined. Figure 4.1 shows the maximum acceleration and the maximum velocity in terms of the relationship with the ratio of the maximum ground response (G. L.: -2 m/G. L.: -35 m) to the input motion levels (G. L.: -35 m). It can be seen that amplification decreased with greater input motion.

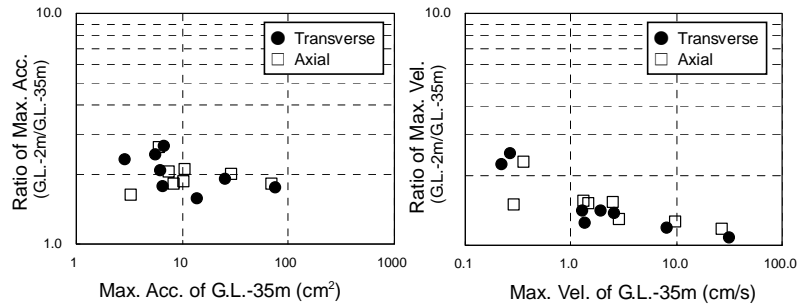


**Figure 4.1** Relationship between input motion and maximum response of surface ground

Figure 4.2 (a) shows the relationship between the maximum acceleration at G. L. -35 m and the ratio of the maximum embankment acceleration to that at the G. L. -35 m depth used as the base. Figure 4.2 (b) shows the results obtained when the maximum acceleration at Point c was set as the base. It can be considered that the former figure shows the response of the embankment in reference to the ground, and that the latter shows the response of the embankment alone. As the amplification of the embankment alone is smaller than that of the ground-embankment system, embankment behavior is considered to be affected by ground behavior (Nishimoto et al., 2008). The figures also indicate that amplification decreases with higher values of maximum acceleration input to the embankment for both bases.

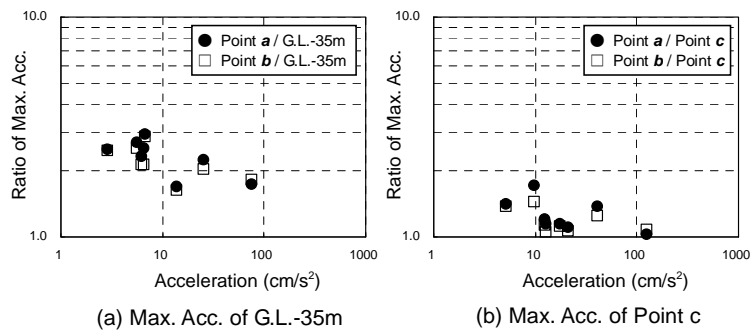


**Figure 4.2** Relationship between input motion and maximum acceleration response for an embankment (transverse to embankment axis)

### 4.2. Transfer characteristics of the embankment

In Figure 4.3, the transfer functions of the ground surface (G. L.: -2 m) in relation to that underground (G. L.: -35 m) in the embankment axial and transverse directions are shown together for the 2003 Tokachi-Oki Earthquake (Eq13) and for the 1997 Urakawa-Oki Earthquake (Eq09; an example of a relatively small earthquake). Figure 4.4 shows the transfer function at Point b in relation to that at G. L. -35 m for Eq09 and Eq13. Figure 4.5 shows the transfer functions of Points a and b in the

embankment transverse direction in relation to that at Point c.

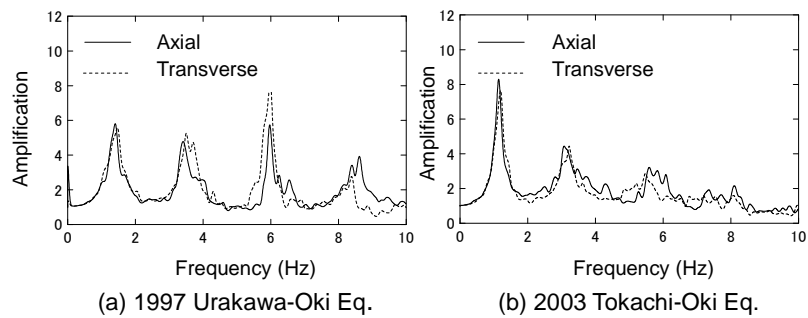


**Figure 4.3** Comparison of transfer function of surface ground (Site B)

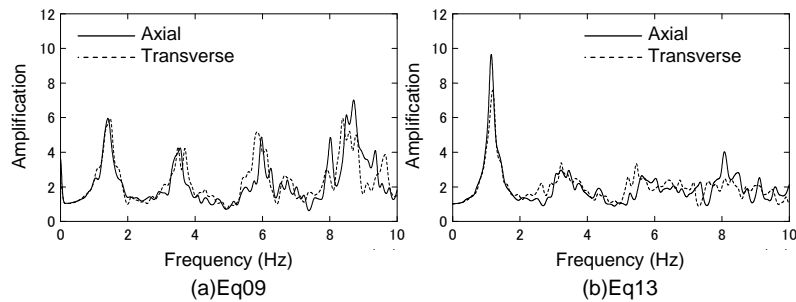


**Figure 4.4** Transfer function of an embankment crest relative to its base (Point b/G.L.-35m)

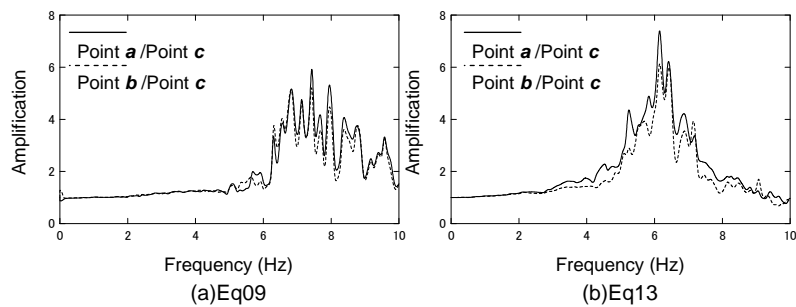


**Figure 4.5** Transfer function of an embankment (Point a/Point c, Point b/point c)

Unlike the case for the embankment alone (the transfer function in relation to Point c), the transfer function of the ground-embankment system has four peaks in a range between 0 Hz and 10 Hz. The function of the ground-embankment system is similar to that of the ground, and their values for low-order peak frequencies are almost the same. Accordingly, the behavior of the ground-embankment system is considered to be controlled by ground behavior within the range of the earthquake motion levels examined in this study.

In regard to the transfer function of the embankment alone, amplification increased in a range from 6 Hz to 8 Hz for Eq09, while it peaked at 6 Hz for Eq13. Considering that the natural frequency of the ground at Site B is approximately 1.2 – 1.3 Hz (Nishikawa et al., 2002, Nishimoto et al., 2006), it is believed that the amplitude in this frequency range reflected the natural frequency of the embankment.

Figure 4.6 shows the relationship between input motion levels and peak frequency for the ground-embankment system and for the embankment alone. The input motion level for the former was at G. L. -35 m, and that for the latter was at Point c. The peak frequency is the predominant frequency of the transfer function at Point b in relation to that at G. L. -35 m for the ground-embankment system, and the predominant frequency of the transfer function at Point b in

relation to that at Point c for the embankment alone. For the ground-embankment system, data for the first to the third peak frequencies are shown; for the embankment alone, data for only the first peak frequency are shown.

The figures indicate that the peak frequency decreased as the input motion level increased. The ratio of decrease in the first peak frequency for the ground-embankment system was approximately 0.81 in the transverse direction.

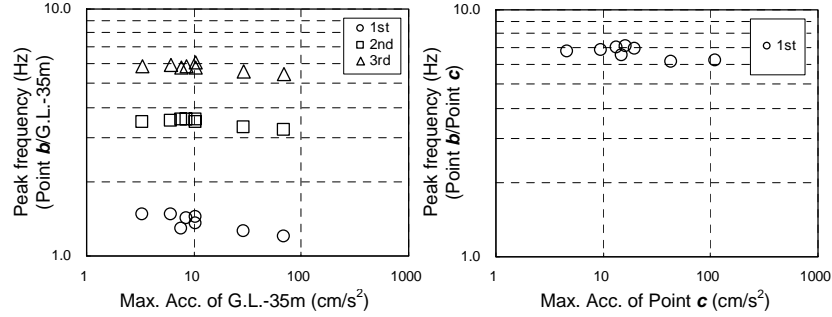


**Figure 4.6** Relationship between input motion and peak frequency (transverse to embankment axis)

Assuming that the first mode is predominant for the seismic behavior of the ground, the predominant period and frequency can be expressed by Equation (4.1) using the quarter wavelength law (Nishimoto et al., 2008):

$$T = \frac{1}{f} = \frac{4H}{V_s} \quad (4.1)$$

Here,  $T$  is the predominant period (s),  $f$  is the predominant frequency (Hz),  $H$  is the layer thickness (m), and  $V_s$  is the shear wave velocity (m/s). The predominant frequencies for a strong and a weak earthquake (indicated by  $f_s$  and  $f_w$ , respectively) can be expressed as Equations (4.2) and (4.3) by replacing  $V_s$  with  $G$  on the basis of  $G = \rho V_s^2$  and using shear modulus for a strong earthquake  $G_s$  and for a weak earthquake  $G_w$ :

$$f_s = \frac{1}{4H} \sqrt{\frac{G_s}{\rho}} \quad (4.2)$$

$$f_w = \frac{1}{4H} \sqrt{\frac{G_w}{\rho}} \quad (4.3)$$

These equations can be rewritten in terms of  $G$  as follows:

$$G_s = f_s^2 (4H)^2 \rho \quad (4.4)$$

$$G_w = f_w^2 (4H)^2 \rho \quad (4.5)$$

Accordingly, a reduction in shear modulus during the earthquakes of  $G^*$  can be expressed by Equation (4.6) using predominant frequencies for strong and weak earthquakes:

$$G^* = \frac{G_s}{G_w} = \left( \frac{f_s}{f_w} \right)^2 \quad (4.6)$$

It can be estimated that the ratio of reduction in the shear modulus of the ground-embankment system in an earthquake is approximately 0.6 – 0.7 based on the ratio of decrease in the first peak frequency as calculated using Equation (4.6). Considering that the ratio of decrease in ground shear modulus during a strong earthquake at Site B is approximately 0.64 (Nishimoto et al., 2006), the reduction of modulus for the ground-embankment system is almost the same level as that for the ground. The behavior of the ground-embankment system is therefore considered to be controlled by ground behavior within the earthquake motion levels examined in this study.

As shown in Fig. 10, the transfer functions of the embankment demonstrate that the predominant frequency decreases as the input motion level increases. The peak frequency for the embankment was not as distinguishable as that for the ground-embankment system, and identification of the first peak frequency is difficult. However, assuming that the peak frequency for a weak earthquake (Eq09) and a strong earthquake (Eq13) are 7.0 Hz and 6.2 Hz, respectively, the ratio of decrease in shear modulus will be approximately 0.78. Based on this, it is presumed that the shear modulus of the embankment alone will also decrease. The ratio of decrease in shear modulus is further considered to be smaller than that for the ground-embankment system.

**4.3. Stress-shear strain characteristics of the embankment based on observation records**

Acceleration time histories obtained at points *b* and *c* were integrated twice to find displacement time histories. The difference between these two values was used to determine relative displacement, which was divided by the distance (6.0 m) between Point *b* and Point *c* to calculate the average shear strain of the embankment (Nishimoto et al., 2008). Figure 4.7 shows the relationship between effective shear strain and maximum acceleration at Point *c*. Effective shear strain here refers to time-variable shear strain time histories converted to harmonic amplitude values. In this study, effective shear strain was found by multiplying the maximum shear strain time history by 0.65. Effective shear strain at the  $6 \times 10^{-4}$  level occurred during Eq13, in which the earthquake motion at Point *c* was the largest, and that at the  $1.5 \times 10^{-5}$  level occurred even during Eq09, in which the earthquake motion was the smallest.

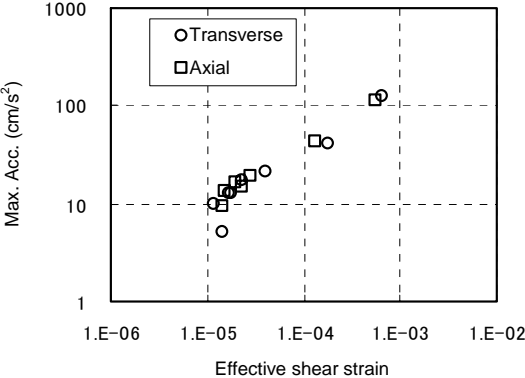


**Figure 4.7** Relationship between effective shear strain and maximum acceleration at Point *c*

Figure 4.8 shows the relationship between effective shear strain and the ratio of decrease in shear modulus calculated from Equation (4.6), where  $f_w$  is the smallest predominant frequency. Nishimoto et al., (2006) points out that ground has a nonlinear characteristic by which shear modulus decreases with higher values of shear strain. It can be seen from the figure that the embankment also had a similar nonlinear characteristic. The figure also shows the results of a dynamic deformation characteristic test performed using samples collected from the embankment. The ratio of decrease in shear modulus is almost the same for the calculation and test results except for the fact that shear modulus as ascertained from the ratio of predominant frequencies began to decrease earlier than that determined from the test results. This difference is considered to stem from issues with accuracy in reading the predominant frequency and the value for effective shear strain being set to 0.65 times the maximum shear strain. Further studies will be conducted to examine this difference based on data

accumulation.

Figure 4.9 shows the relationship between the effective shear strain of the ground and that of the embankment calculated from the relative displacement between G. L. -2 m and G. L. -35 m. For effective ground shear strain exceeding the  $10^{-4}$  level, the value is larger than that for the embankment, but the difference is small. It can be concluded that the shear strain level occurring in the embankment is almost the same as that in the ground.

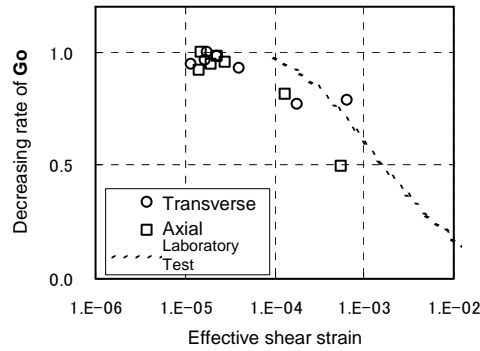


**Figure 4.8** Relationship between effective shear strain and the ratio of decrease in shear modulus

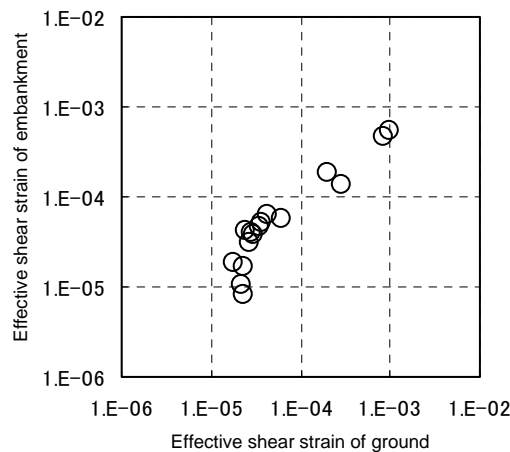


**Figure 4.9** Relationship between the effective shear strain of the ground and that of the embankment

## 5. CONCLUSIONS

Records from the 2003 Tokachi-Oki Earthquake were observed at liquefaction array observation sites in Tomakomai. The analysis of the observed earthquake motion records and past records can be summarized as follows:

- 1) Acceleration values exceeding  $130 \text{ cm/s}^2$  and clear residual excess pore water pressure were recorded in sandy ground at Site B and in the highway embankment at Site C.
- 2) As embankment motion amplification decreased with higher levels of input to the structure, it was concluded that the embankment exhibited nonlinear characteristics.
- 3) The transfer function of the ground-embankment system up to 10 Hz had four distinctive peaks, while that of the embankment had one peak. As the transfer function of the ground-embankment system was similar to that of the ground, low-order vibration modes are considered to be affected by ground vibration modes.
- 4) The peak frequency of the transfer function tended to decrease with higher input levels. Assuming that the first-mode behavior of the ground-embankment system is predominant, the

ratio of decrease in the shear modulus of the ground-embankment system during strong earthquakes was estimated based on the ratio of decrease in the first peak frequency. The results showed that the ratio of reduction became approximately 0.6 – 0.7. Similarly, the ratio of decrease in shear modulus of the embankment alone was considered to be approximately 0.78.

- 5) As with the ground, the embankment showed nonlinear behavior in which shear modulus decreased with higher values of shear strain. The shear strain level in the embankment was slightly smaller than that in the ground.

## REFERENCES

- Hayashi, H., Nishikawa, J., Egawa, T., Miwa, S. and Ikeda, T. (2000). Ground Seismic Behavior from Liquefaction Array Observation. *12th World Conference on Earthquake Engineering*. No. 517.
- Nishikawa, J., Hayashi, H., Egawa, T., Miwa, S. and Ikeda, T. (2001). Evaluation of the Seismic Behavior on Sandy Ground with Built-up Pore Water Pressures by Effective Stress Analysis. *4th International Conference on Recent Advances in Geotechnical Earthquake Engineering and Soil Dynamics*, paper No. 3.29.
- Nishikawa, J., Hayashi, H., Egawa, T., Miwa, S. Ikeda, T. and Mori, S. (2002). Liquefaction Array Observations at Two Sites and Analysis of their Records. *Journals of JSCE*. **No. 703: 1-59**, 327 – 343 (in Japanese).
- Nishimoto, S., Miwa, S. and Ikeda, T. (2006). Strong Motion of Records at the Tomakomai Liquefaction Array during the 2003 Tokachi-Oki Earthquake. *First European Conference on Earthquake Engineering and Seismology*, paper No. 471.
- Nishimoto S, Ikeda T, Kamiakito N and Miwa S. (2007). Investigation on Seismic Behavior of a Road Embankment on Soft Ground Based on Earthquake Observation Records. *4th International Conference on Earthquake Geotechnical Engineering*, paper No. 1335.
- Nishimoto, S., Hashimoto, H., Ikeda, T., Miwa, S. and Kamiakito, N. (2008). Seismic Behavior of a Road Embankment on Soft Ground Based on Earthquake Observations. *Journals of JSCE*. **C-Vol. 64: No. 4**, 802 – 812 (in Japanese).
- Nishimoto, S. and Ikeda, T. (2009). Seismic Behavior of a Road Embankment on Soft Ground during the 2003 Tokachi-Oki Earthquake. *Earthquake Geotechnical Engineering Satellite Conference, XVIIth International Conference on Soil Mechanics & Geotechnical Engineering*, paper No. 15.